International Journal of Biochemistry and Cell Biology 112 (2019) 79–87

Contents lists available at ScienceDirect

International Journal of Biochemistry and Cell Biology

journal homepage: www.elsevier.com/locate/biocel

Heat shock protein family B member 1 facilitates ezrin activation to control cell migration in esophageal squamous cell carcinoma

Ying-Hua Xie[a,b], Li-Yan Li[a,b], Jian-Zhong He[a,b], Xiu-E Xu[a,c], Lian-Di Liao[a,c], Qiang Zhang[a,b], Jian-Jun Xie[a,b], Li-Yan Xu[a,c,**], En-Min Li[a,b,*]

[a] The Key Laboratory of Molecular Biology for High Cancer Incidence Coastal Chaoshan Area, Shantou University Medical College, Shantou 515041, Guangdong, PR China
[b] Department of Biochemistry and Molecular Biology, Shantou University Medical College, Shantou 515041, Guangdong, PR China
[c] Institute of Oncologic Pathology, Shantou University Medical College, Shantou 515041, Guangdong, PR China

ARTICLE INFO

Keywords:
Ezrin
HSPB1
Activation
Migration
Esophageal squamous cell carcinoma (ESCC)

ABSTRACT

Ezrin plays an important role in the development and progression of human esophageal squamous cell carcinoma (ESCC), providing a link between the cortical actin cytoskeleton and the plasma membrane to govern membrane structure and protrusions. However, the mechanism by which ezrin is activated still remains unknown in ESCC. Here, we identify a novel interaction between ezrin and heat shock protein family B (small) member 1 (HSPB1) in ESCC cells by mass spectroscopy and co-immunoprecipitation. HSPB1 only interacts with inactive ezrin and binds to the α-helical coiled coil region of ezrin. Knockdown of HSPB1 resulted to the decline of phosphorylation at ezrin Thr567, markedly suppressing the ability of ezrin to bind to the actin cytoskeleton and migration of ESCC cells. Furthermore, neither the constitutively active phosphomimetic ezrin T567D, nor inactivated ezrin T567A could restore cell migration following HSPB1 knockdown. Low HSPB1 expression was associated with favorable overall survival of ESCC patients. Taken together, HSPB1, as an important partner, participates in the activation of ezrin and merits further evaluation as a novel therapeutic target against human ESCC.

1. Introduction

Ezrin is a member of the ezrin-radixin-moesin (ERM) family of proteins that act as linkers between the actin cytoskeleton and the plasma membrane. ERM proteins are highly homologous and share a similar structure, including an N-terminal FERM (Four point one, ERM) domain that binds the plasma membrane, a C-terminal ezrin-radixin-moesin association domain (C-ERMAD) that can attach to actin filaments, and an α-helical region that links the C-ERMAD and the FERM domain(Gould et al., 1989). The C-ERMAD domain can bind to the FERM domain of the same molecule to form a monomer, or with another ERM molecule to form a homodimer or heterodimer (Pearson et al., 2000; Gary and Bretscher, 1995). This reversible head to tail interaction leads to a closed conformation and the masking of both the membrane and actin binding sites, resulting in inactivation of the ERM protein. Activation of ERM proteins requires an open conformation, which is achieved by binding to phosphatidylinositol 4,5-bisphosphate (PIP2) to uncouple the C-terminal domain from the FERM domain, and kinase-mediated phosphorylation at the conserved threonine residues (T567, T564 and T558, for ezrin, radixin and moesin, respectively) (Fievet et al., 2004).

Ezrin plays an important role in the development and progression of various human cancers, regulating cytoskeletal rearrangements, cell migration, and cell invasion. Our previous studies have found that ezrin is associated with poor prognosis of patients with esophageal squamous cell carcinoma (ESCC) (Xie et al., 2011). We also found that the interaction of lncRNA EZR-AS1 with SMYD3 enhances transcription of the EZR gene in ESCC cells (Zhang et al., 2018). However, the mechanism by which ezrin is activated still remains unknown in ESCC.

Here, we report the discovery of a novel interaction between ezrin

Abbreviations: C-ERMAD, C-terminal ezrin-radixin-moesin association domain; DAPI, 4′6-Diamidino-2-phenylindole dihydrochloride; DFS, Disease-free survival; EGF, epidermal growth factor; ERM, ezrin-radixin-moesin; ESCC, esophageal squamous cell carcinoma; FERM, Four point one ERM; HSPB1, heat shock protein family B member 1; IHC, immunohistochemistry; OS, overall survival; PBS, phosphate buffer saline; PIP2, phosphatidylinositol 45-bisphosphate; RIPA, radio-immunoprecipitation assay; TMA, tissue microarrays; WT, wild type

* Corresponding author at: Department of Biochemistry and Molecular Biology, Shantou University Medical College, Shantou 515041, Guangdong, PR China.
** Corresponding author at: The Key Laboratory of Molecular Biology for High Cancer Incidence Coastal Chaoshan Area, Shantou University Medical College, Shantou 515041, Guangdong, PR China.
E-mail addresses: lyxu@stu.edu.cn (L.-Y. Xu), nmli@stu.edu.cn (E.-M. Li).

https://doi.org/10.1016/j.biocel.2019.05.005
Received 4 January 2019; Received in revised form 6 May 2019; Accepted 8 May 2019
Available online 10 May 2019

Table 1
Mass spectrometry analysis of ezrin-interacting proteins.

Protein ID	Gene and protein	Vector prot_score	Ezrin-STrEP prot_score	-EGF prot_score	+EGF prot_score
IPI100843975	EZR Ezrin	896	1291	2935	3165
IPI100219365	MSN Moesin	312	415	1052	823
IPI100903145	ROX Radixin		305	822	697
IPI100025512	HSPB1			197	121
IPI100893541	PDIA3			110	
IPI100419585	PPIA			85	77
IPI100456492	CROCC			72	122
IPI100443909	CNPY2			68	
IPI100479997	STMN1			64	
IPI100396378	HNRNPA2B1			60	
IPI100000874	PRDX1			60	
IPI100216318	YWHAB			51	
IPI100397801	FLG2				55

and heat shock protein family B (small) member 1 (HSPB1). HSPB1 interacts with inactive ezrin and facilitates ezrin activation to control cell migration in ESCC. Low expression of HSPB1 is associated with favorable overall and disease-free survival of ESCC patients, revealing that HSPB1 is a potential target for future ESCC treatment.

2. Material and methods

2.1. Plasmids and siRNAs

Wild type (WT) HSPB1 was cloned into a plasmid encoding a 3×Flag epitope, and the coding region of ezrin was amplified and cloned into the pcDNA3-HA, pcDNA3-VSVg, pcDNA3-StrEP and pEGFP-N1 vectors. A Fast Mutagenesis System kit (TransGen Biotech, Beijing) was used to generate site-specific mutations at ezrin K60, S66, K79, Y146, Y354, T567, K253/254, K262/263 according to the manufacturer's manual. Ezrin 1-300aa, ezrin 300-586aa and ezrin 478-586aa constructs were individually cloned into the pcDNA3-HA vector. All constructs were confirmed by sequencing. siRNA targeting HSPB1 was synthesized by GenePharma (Suzhong, Jiangsu, China), and contained the following sequence: 5′- CCCUGGAUGUCAACCACUUTT-3

2.2. Cell Culture and transfection

Details of cell lines used in this study have been described previously (Lv et al., 2014). The KYSE150, KYSE140, KYSE510, TE3 and SHEEC esophageal squamous carcinoma cell lines were cultured in Roswell Park Memorial Institute (RPMI) 1640 medium (HYCLONE, USA) with 10% fetal bovine serum (Invitrogen Life Technologies). EC109, KYSE450 and 293 T cells were cultured in Dulbecco's modified Eagle's medium (GIBCO) supplemented with 10% new-born bovine serum (Excell Biology Inc). Plasmid and siRNA transfections were performed with Lipofectamine 3000 reagent (Invitrogen Life Technologies) and Lipofectamine® RNAiMAX Transfection Reagent (Invitrogen Life Technologies), respectively. All cells were incubated at 37 °C in a humidified atmosphere containing 5% CO_2. Cells were tested to ensure they were mycoplasma-negative.

2.3. Mass spectrometry

Mass spectrometry was performed as described previously (He et al., 2017). For the active group (+EGF), EC109 cells were starved in serum-free medium for 11 h after transfection with the ezrin-STrEP plasmid for 48 h, and then treated with epidermal growth factor (EGF, final concentration 50 ng/mL) for 1 h to activate ezrin. In the starvation group (-EGF), cells transfected with ezrin-STrEP were starved in serum-free medium for 12 h. In the negative control group, cells were transfected with STrEP and were treated the same as the experimental group. Total cell lysates were subjected to STrEP-targeted column chromatography, and then the target protein was prepared for mass spectrometry analyses.

2.4. Co-immunoprecipitation

Co-immunoprecipitation assay has been described previously (He et al., 2017). KYSE150 cells were transfected with or without plasmids for 48 h and then the cells were lysed in radio-immunoprecipitation assay (RIPA) lysis buffer containing 1× complete protease inhibitor cocktail (Thermo Fisher). The corresponding antibodies were incubated with Protein A/G PLUS-Agarose (sc-2003, Santa Cruz) for 1 h at 4 °C, and then protein lysate was added and incubated overnight at 4 °C. After four washes in immunoprecipitation buffer, the immunoprecipitates were examined by Western blotting.

2.5. Immunofluorescence and immunohistochemistry

Immunofluorescence was performed as previously described (Zhang et al., 2018). In detail, KYSE150 cells transfected with or without ezrin-pEGFP (WT, T567A or T567D) were fixed with 4% paraformaldehyde for 10 min at room temperature. After washing with cold phosphate buffer saline (PBS), the cells were permeabilized in 0.1% Triton X-100 in PBS for 8 min on the ice and blocked for 1 h in PBS containing 5% donkey serum at room temperature, and then incubated with primary antibodies (ezrin, E1281, Sigma, 1:400; pezrin-T567, 3726S, Cell Signaling Technology, 1:200) at 4 °C overnight. The cells were incubated for 1 h at room temperature with secondary antibodies (Alexa Fluor® 488-conjugated donkey anti-rabbit IgG (H + L), 711-545-152, Jackson ImmunoResearch Laboratories, 1:200) or HSP27 antibody (F-4) Alexa Fluor® 647 (sc-13132 AF647, Santa Cruz, 1:200), followed by washing with PBS. Nuclei were then counterstained with 4′,6-Diamidino-2-phenylindole dihydrochloride (DAPI) (D9542, Sigma, 1:2000). Slides were viewed using a confocal microscope (LSM880, Carl Zeiss Micro-Imaging) with a 40×, 1.43 NA, oil-immersion objective lens. Colocalization analysis was performed with Fiji, which was an image processing package ImageJ (National Institutes of Health, USA). Pearson's Correlation Coefficient (above threshold) was showed to examine the colocalization.

The data set of formalin-fixed, paraffin-embedded tissue specimens were obtained from ESCC patients undergoing curative resection at the Shantou Central Hospital, including 265 patients treated during November 2007 to January 2010. All specimens were confirmed as ESCC by pathologists in the Clinical Pathology Department of the hospital. Ethical approval was obtained from the ethical committee of the Central Hospital of Shantou City and the ethical committee of the Medical College of Shantou University. Only resected samples from surgical patients with written informed consent were included.

Tissue microarrays (TMA), immunohistochemistry (IHC) and evaluation of IHC variables were performed as described previously (Liu

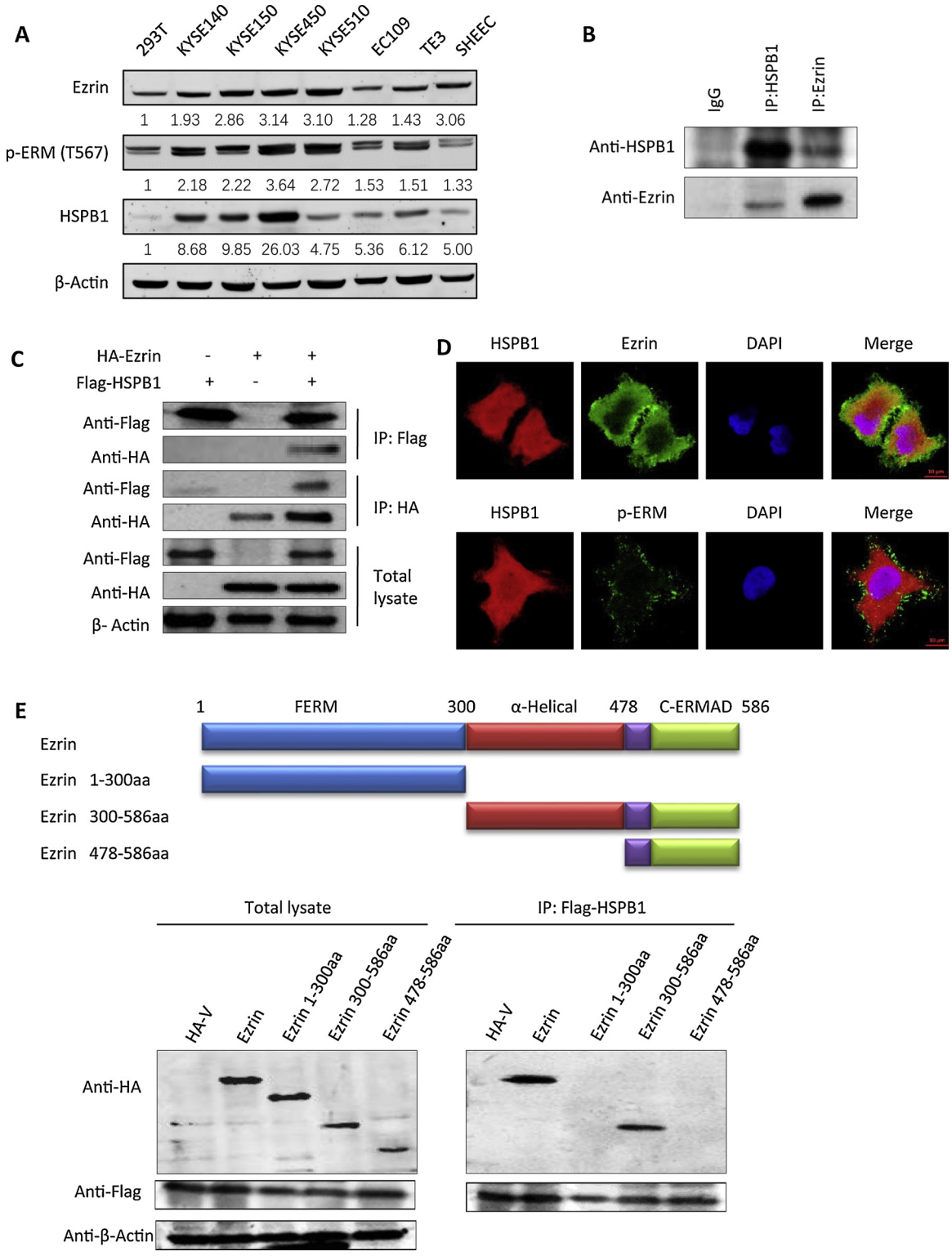

Fig. 1. Identification of interaction between ezrin and HSPB1. (A) Ezrin and HSPB1 expression and phosphorylation level in ESCC cells. Western blotting of cell extracts was used to probe for total ezrin, phosphorylated ezrin (p-ERM (T567)) and HSPB1. The optical density analysis data of ezrin, p-ERM (T567) and HSPB1 were first quantified by beta-actin, and then normalized by 293 T cells. Quantitative data was displayed below the image. (B) Co-IP identifies the interaction of endogenous ezrin with HSPB1. After routine culture of KYSE150 cells for 48 h, cells were lysed in RIPA buffer to extract total cellular protein and co-IP experiments were performed with HSPB1 and ezrin antibodies, respectively. (C) Co-IP shows exogenous HA-ezrin and Flag-HSPB1 interact. KYSE150 cells were co-transfected with HA-ezrin and Flag-HSPB1 plasmids, and HA and Flag empty plasmids were used as controls. After 48 h following transfection, co-IP experiments were performed using Flag antibodies and HA antibodies. (D)Typical immunofluorescence images of HSPB1 (red) and ezrin (green) or p-ERM (T567) (green) in KYSE150 cells. Scale bars, 10 μm. (E) HSPB1 binds to the alpha-helical region of ezrin. The full-length and truncated plasmids of HA-tagged ezrin were co-transfected with Flag-HSPB1 in KYSE150 cells, and co-IP experiments were performed using Flag antibody. (For interpretation of the references to colour in this figure legend, the reader is referred to the web version of this article).

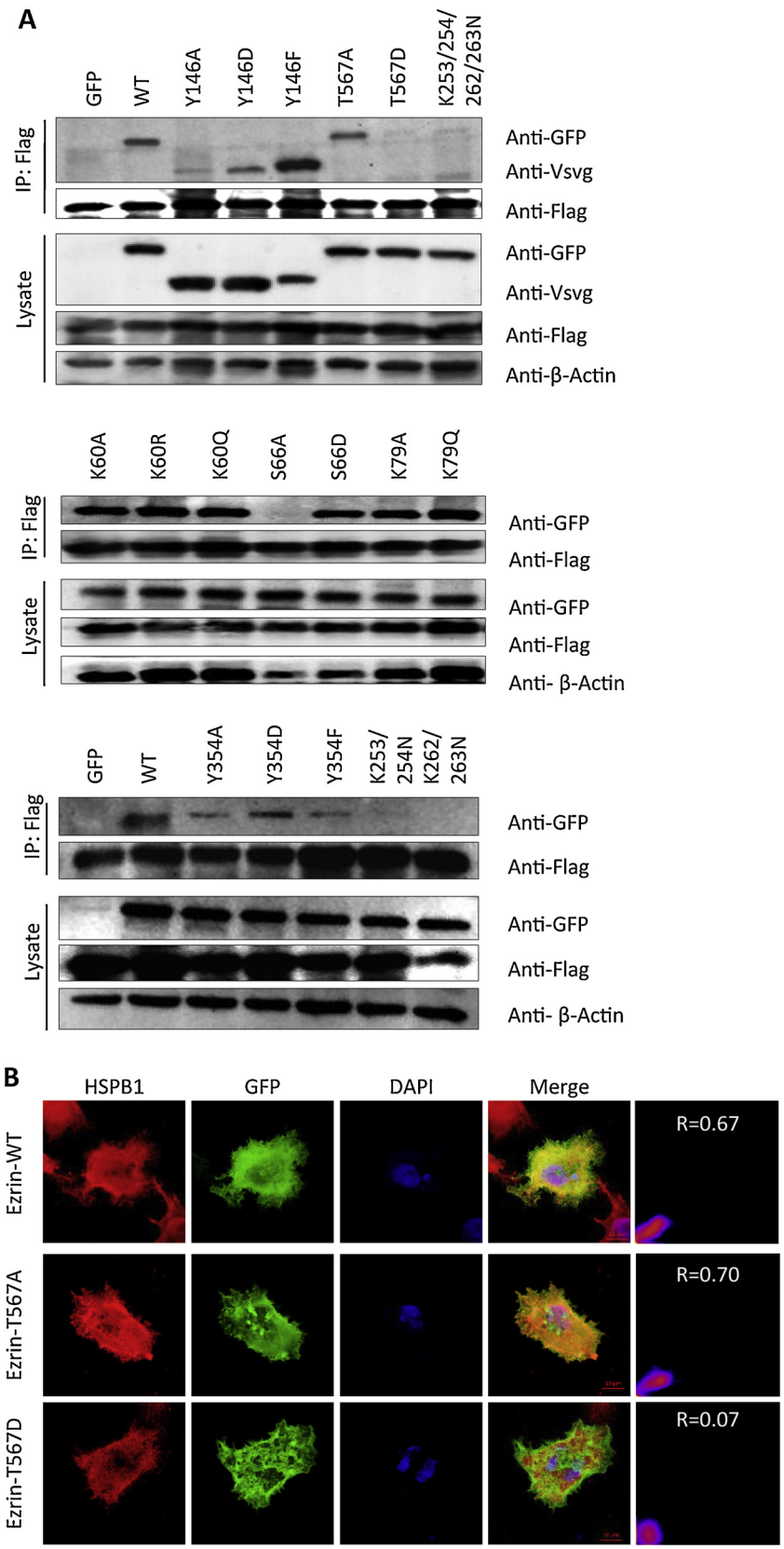

Fig. 2. The effect of ezrin key amino acid sites on the interaction between ezrin and HSPB1. (A) The KYSE150 cell line was transfected with the mutated plasmids of each key site in ezrin (phospho-mimicking mutation S66D, Y146D, Y354D, T567D, non-phosphorylatable S66A, Y146A, Y146F, Y354A, Y354F, T567A, acetylation mutation K60Q, K79Q, deacetylation mutation K60A, K60R, K79A, and mutation of lysines to asparagines K253/254N, K262/263N and K253/254/262/263 N, which destroyed ezrin FERM domain binding to PIP2). RIPA was used to extract total protein, and co-IP was used to identify the interactions. (B) Ezrin-WT/T567A/T567D plasmids were transfected into the KYSE150 cell line, and the co-localization with endogenous HSPB1 in each group was detected by immunofluorescence. R, Pearson's Correlation Coefficient, was used to evaluate co-localization of HSPB1 and ezrin mutants.

et al., 2018; Xie et al., 2011). Overall survival (OS) was measured from the date of surgery to death or the latest follow-up. Disease-free survival (DFS) was measured from the date of surgery to the first occurrence of any of the following events, including recurrence, distant metastasis or death from any cause without documentation of a cancer-related event.

We scored the expression of HSPB1 with a newly emerged technology for extracting the H score automatically. H score was evaluated by an automated quantitative pathology imaging system (Perkin Elmer, Waltham, MA, USA), producing a continuous protein expression value in the range of 0 to 300. According to the expression of HSPB1, X-tile

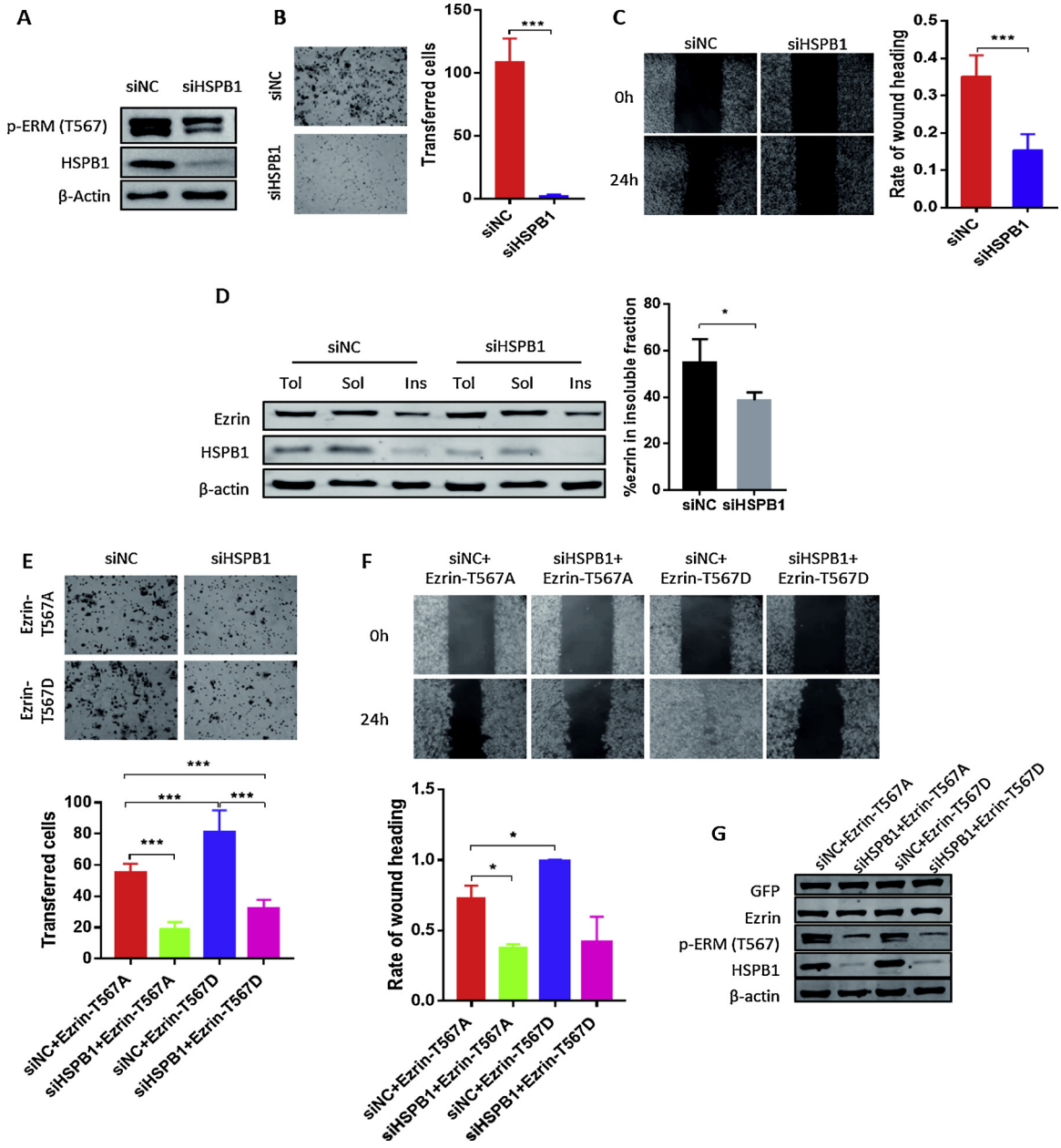

Fig. 3. HSPB1 facilitates ezrin activation to control cell migration in ESCC. (A) The effect of HSPB1 knockdown on ezrin phosphorylation. Western blot analyzed the expressions of p-ERM (T567), HSPB1 and β-actin when HSPB1 was knockdown or not. (B and C) Analysis of transwell and wound-healing show that the effect of HSPB1 knockdown reduces cell migration in KYSE150. (D) A similar amount of total (Tot), soluble (Sol) or insoluble (Ins) cell fractions were analyzed by Western blotting with ezrin, HSPB1 and β-actin antibodies. The optical density analysis data of ezrin relative to β-actin were used to evaluate the percentage of ezrin in insoluble fraction to total ezrin. (E and F) Overexpression of activated ezrin partially restores the inhibitory effect of HSPB1 knockdown on cell migration. KYSE150 cells were transfected with siHSPB1 and ezrin T567A or T567D. Cell migration was measured by transwell migration and wound healing. (G) Representative immunoblotted images of ezrin, p-ERM (T567), HSPB1, β-Actin and ezrin-T567A/T567D (with GFP label) expression in (E) and (F). The unpaired *t* test was used to determine the significance of differences between groups and data was obtained in at least three independent experiments in (B), (C), (E) and (F). Average values are given ± SD. *, $P < 0.05$; ***, $P < 0.005$.

(Camp et al., 2004) version 3.6.1 was used to find the best cutting point for dividing the tumors into two subsets (HSPB1 low-expression and HSPB1 high-expression).

2.6. Western blot analysis

Western blots were performed as described previously (Xie et al., 2010). Total cell lysates were prepared from confluent cultures in Laemmli sample buffer (161-0737, Bio-Rad). Blots were incubated with primary antibodies against ezrin (MS-661-P, NeoMarkers, 1:1000), HSPB1 (sc-13132, Santa Cruz, 1:1000), p-ERM (T567) (3726S, Cell Signaling Technology, 1:1000), GFP (sc-9996, Santa Cruz, 1:1000), and β-actin (sc-47778, Santa Cruz, 1:2000). Appropriate HRP-conjugated secondary antibodies were from Santa Cruz Biotechnology (Santa Cruz, 1:5000). Signals were detected, with luminol reagent, using a ChemiDoc Touch (Bio-Rad Laboratories, Inc., Hercules, CA, USA). Densitometric analysis was performed with Image Lab software Version 2.0 (Bio-Rad Laboratories, Inc., Hercules, CA, USA).

2.7. Migration assay

Cell migration was assessed using transwell and wound-healing

Table 2
The correlation between HSPB1 and clinicopathological characteristics in ESCC.

Variables	HSPB1[a]		chi-square value	R	*P*[*]
	Low	High			
Age (year)					
≤58	122	12	1.974	0.060	0.184
> 58	112	19			
Gender					
Male	46	8	0.638	−0.049	0.476
Female	188	23			
Therapies					
Only Surgery	129	19	0.605	−0.037	0.895
Postoperative Chemotherapy	31	4			
Postoperative Radiotherapy	51	5			
Others[b]	23	3			
Tumor size					
≤3cm	56	7	0.691	−0.021	0.708
3-5cm	111	17			
> 5cm	67	7			
Tumor location					
upper	12	2	0.401	0.017	0.818
middle	104	12			
lower	118	17			
Histologic grade					
G1	33	5	0.223	−0.028	0.894
G2	181	24			
G3	20	2			
Invasive depth					
T1 + T2	50	9	0.929	−0.059	0.360
T3 + T4	184	22			
Lymph node metastasis					
N0	124	16	3.048	0.061	0.384
N1	62	5			
N2	36	7			
N3	12	3			
pTNM-stage					
I	18	3	0.452	0.011	0.798
II	120	14			
III	96	14			

[*] Fisher's Exact Test; *P* value < 0.05 was considered significant.
[a] low, < 255 scores; high, ≥255 scores.
[b] Preoperative and Postoperative Chemotherapy (2 cases), Preoperative Radiochemotherapy (2 cases) and Postoperative Radiochemotherapy (24 cases).

assays, which were performed as described previously (Zeng et al., 2017). Briefly, KYSE150 cells were transfected with siRNA targeting HSPB1, or a mixture of siRNA and ezrin-T567A or ezrin-T567D, and then cells were starved in serum-free medium for 12 h after being transfected for 36 h. For the transwell assay, 5×10^4 cells were added into the upper transwell chamber (353097; BD Biosciences) in serum-free medium, while 1640 medium with 10% fetal bovine serum was added to the lower chamber. The chambers were incubated for 48 h at 37 °C, and subsequently, the cells that had traversed the membrane to the lower side were fixed with fixative (methanol:acetic acid = 3:1) and then stained with hematoxylin at room temperature for 30 min. Cells in the bottom of the chamber were then counted under a microscope (magnification, ×200). In the wound-healing assay, a scratch was made across the monolayer using a sterile pipette tip. Wound closure information was imaged at 0, 12 and 24 h with a microscope (magnification, ×200), respectively. ImageJ 1.43 u (National Institutes of Health, USA) was used to count the number of cells and wound healing area. Data obtained from 10 different scans were shown as mean values. Data obtained from 10 different scans were shown as mean values. Experiments were repeated twice with similar results.

2.8. Analysis of detergent soluble and insoluble fractions

Analysis of detergent soluble and insoluble fractions was performed as described previously (Fievet et al., 2004; Li et al., 2017). In KYSE150 cells, cellular fractions were obtained from confluent cultures in 6-well plates. Total cellular fractions were collected with Laemmli buffer at 100 °C. Soluble fractions were prepared by a 1 min extraction with 0.5% Triton X-100 buffer (50 mM MES, 3 mM EGTA, 5 mM MgCl2, 0.5% Triton X-100, pH 6.4) at 20 °C and supplemented with 4× Laemmli buffer. The insoluble fractions were extracted with Laemmli buffer at 100 °C. Samples were analyzed by western blot. Densitometric analysis was performed with Image Lab software Version 2.0 (Bio-Rad Laboratories, Inc., Hercules, CA, USA).

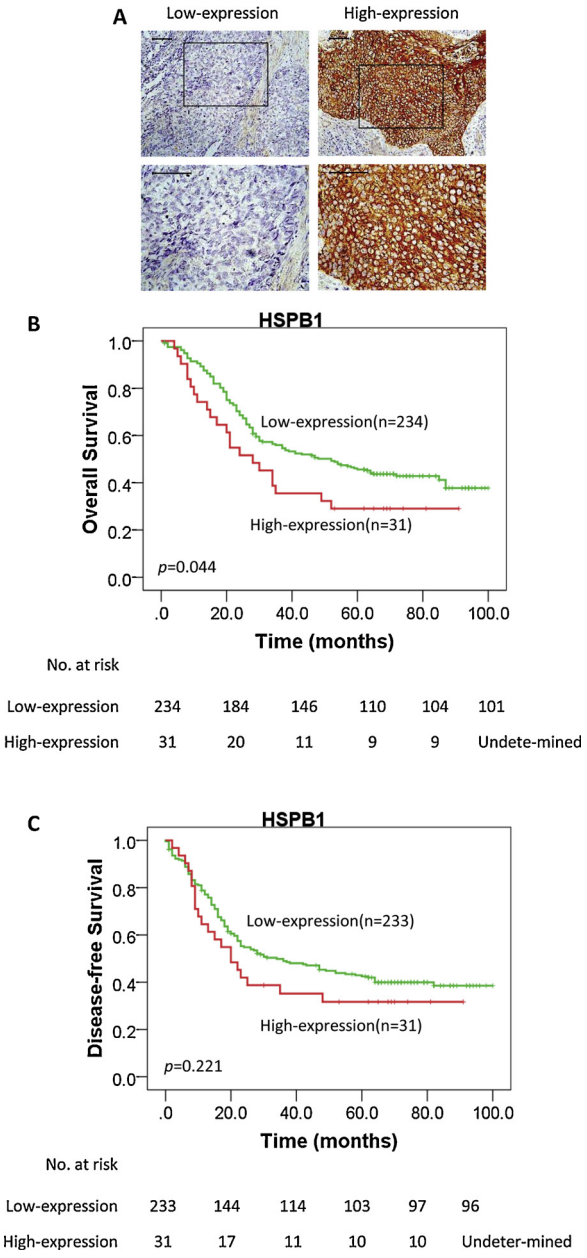

Fig. 4. Overall and disease-free survival in patients with low expression of HSPB1 in ESCC. (A) Typical images of immunohistochemistry of low expression and high expression of HSPB1 in ESCC. A score of less than 255 was defined as a low expression of HSPB1, whereas a score greater than or equal to 255 was considered a high expression. Bars, 50 μm. (B) Kaplan-Meier survival analysis of the relationship between HSPB1 expression and the overall survival of patients with ESCC. (C) Kaplan-Meier survival analysis of the relationship between HSPB1 expression and tumor-free survival in patients with ESCC. A *p* value of less than 0.05 was considered statistically significant.

2.9. Statistical analysis

Data analysis of cell migration was performed using GraphPad Prism 7 software (GraphPad Software, Inc., La Jolla, CA, USA). The unpaired *t* test was used to determine the significance of differences between groups. Data were plotted as mean ± SD, for at least three independent experiments. Kaplan-Meier curves were constructed for overall survival and disease-free survival analysis using a log-rank test and performed with SPSS 13.0 software (SPSS, Inc., Chicago, IL, USA). Correlation analysis was performed using the Fisher's exact probability test. A $p < 0.05$ was deemed statistically significant for all tests.

3. Results

3.1. HSPB1 interacts with ezrin by binding to the α-helical coiled coil region of ezrin in ESCC cells

The EC109 human ESCC cell line was transfected with ezrin-STrEP and treated with EGF to induce ezrin activation. Mass spectrometry analysis showed that ezrin interacted with several proteins in ESCC cells (Table 1). Interestingly, we found a novel ezrin-interacting protein, HSPB1 (heat shock protein family B (small) member 1), which bound to ezrin at a higher intensity in the absence of EGF addition, i.e. the interaction between ezrin and HSPB1 was reduced when cells were treated with EGF to stimulate ezrin activation.

Before further examining the interaction between ezrin and HSPB1, we detected their expression, as well as phosphorylation, in ESCC cell lines (Fig. 1A). Western blot analysis showed that HSPB1, total ezrin and phosphorylation of ezrin T567 site was highly expressed in all ESCC cell lines, compared with the expression in 293 T cells.

To verify the interaction between ezrin and HSPB1, co-immunoprecipitation targeting ezrin or HSPB1 was performed in KYSE150 cells. As predicted, ezrin and HSPB1 co-immunoprecipitated (Fig. 1B), which was also verified by co-immunoprecipitation targeting HA or Flag in KYSE150 cells co-transfected with the HA-ezrin and Flag-HSPB1 plasmids (Fig. 1C). Immunofluorescence staining revealed the partial co-localization of HSPB1 and ezrin in the context region, but there was no co-localization between activated ezrin (p-ERM) and HSPB1 (Fig. 1D). Co-immunoprecipitation showed that only full-length ezrin and ezrin 300-587aa, but not ezrin 1-300aa or 478-586aa, interacted with HSPB1 (Fig. 1E). It can be seen from the schematic diagram of ezrin structure that both full-length ezrin and ezrin 300-587aa contain the α-helical region, while ezrin 1-300aa and 478-586aa do not contain this region. Therefore, we speculated that HSPB1 bound to the α-helical region of ezrin.

3.2. The interaction between HSPB1 and ezrin affects the activation of ezrin

Ezrin post-translational modification regulated the activation of ezrin (Adada et al., 2014). To investigate the effect of interaction between HSPB1 and ezrin on the activation of ezrin, we compared the binding of phosphorylated (ezrin S66D, Y146D, Y354D, and T567D mutants) and non-phosphorylatable ezrin (ezrin S66A, Y146A, Y146 F, Y354A, Y354 F, T567A) to HSPB1. Non-phosphorylatable ezrin T567A, but not phosphorylated ezrin T567D interacted with HSPB1 (Fig. 2A). Contrarily, there was no interaction between phosphorylated ezrin S66D and HSPB1 (Fig. 2A). Ezrin K253/254 and K262/263 are PIP2-binding sites, which are essential for PIP2-induced release of ezrin autoinhibition (Ben-Aissa et al., 2012). We constructed ezrin K253/254 N, K262/263 N and K253/254/262/263 N mutant plasmids to destroyed ezrin FERM domain binding to PIP2, and found that these mutants significantly inhibited the interaction between ezrin and HSPB1 (Fig. 2A). However, acetylation of ezrin seems to have no effect on its interaction with HSPB1, since both acetylation (ezrin K60Q, K79Q) and deacetylation (ezrin K60A, K60R, K79A) of ezrin interacted with HSPB1 (Fig. 2A).

Similar to ezrin WT (wild type), inactivated ezrin (ezrin T567A) and HSPB1 were colocalized with a high colocalization coefficients (Pearson's R value was greater than 0.6), while activated ezrin (ezrin T567D) did not overlap with HSPB1 (Fig. 2B). These data indicate that the interaction of HSPB1 with ezrin affects the activation of ezrin, and only inactive ezrin, but not active ezrin interacts with HSPB1.

3.3. HSPB1 facilitates ezrin activation to control cell migration in ESCC cells

As a membrane-cytoskeleton linker, ezrin plays an important role in regulation of many cellular processes, such as cancer cell migration. Our results prompted us to investigate whether HSPB1 facilitates ezrin activation and alters the biological behavior of ESCC cells. We used siRNA-mediated knockdown to exogenously manipulate expression of HSPB1. Decreasing HSPB1 expression suppressed ezrin phosphorylation (Fig. 3A), as well as migration of KYSE150 cells (Fig. 3B and C). To assess the ability of ezrin to associate with the actin cytoskeleton while HSPB1 was knocked down, Triton X-100 fractionation was used to preserve the cytoskeleton and cytoskeleton-associated proteins. Quantification after western blot analysis of soluble and insoluble fractions confirmed that ezrin was less insoluble when HSPB1 was knocked down (54.6% of ezrin in insoluble fraction in siNC group, and 38.6% in siHSPB1 group, $p < 0.05$, Fig. 3D). This indicates that the absence of HSPB1 weakens the ability of ezrin to bind to the actin cytoskeleton. We next investigated whether active ezrin could recover migration in HSPB1 knockdown cells. Transwell and wound-healing assays showed that, compared to inactivated ezrin (ezrin-T567A), constitutively-active ezrin (ezrin-T567D) promoted cell migration (comparison between the siNC + ezrin-T567A vs. siNC + ezrin-T567D groups, Fig. 3E and F). However, once HSPB1 was knocked down, cell migration was significantly inhibited and could not be recovered by either constitutively-active or inactivated ezrin (comparison between the siNC + ezrin-T567A vs. siHSPB1 + ezrin-T567A groups, as well as siNC + ezrin-T567D vs. siHSPB1 + ezrin-T567D groups), suggesting that HSPB1 is necessary for ezrin to promote cell migration. In order to eliminate the interference of mutations on the results, we transfected plasmid encoding wildtype ezrin (ezrin-GFP), and found that, similar to ezrin-T567A and ezrin-T567D, ezrin WT could not restore cell migration from HSPB1 knockdown (Supplementary Figure S1). Western blot analysis showed that HSPB1 knockdown reduced ezrin phosphorylation at T567, but did not affect the expression of ezrin (Fig. 3G).

3.4. Low expression of HSPB1 is associated with better prognosis of ESCC patients

Our earlier study found that ezrin expression is related to poor overall survival of ESCC patients, but the clinical significance of HSPB1 remained unknown. We analyzed the gene expression microarrays of 265 ESCC cases, and detected the expression of HSPB1 by immunohistochemistry. We investigated the relationship between HSPB1 expression and the clinicopathological characteristics of the ESCC patients and found the expression of HSPB1 was not related to the histologic grade, invasive depth or other clinicopathological characteristics (Table 2). Kaplan-Meier analysis were used to evaluate the relationship between HSPB1 expression and survival of ESCC patients. We found that low expression of HSPB1 was associated with better overall survival ((Fig. 4A–C). Patients with low expression of HSPB1 had a 5-year survival of 45.6%, compared with 29.0% for HSPB1-overexpressing patients ($p = 0.044$). Similarly, the 5-year disease-free survival of patients with low expression of HSPB1 was 45.6%, while that of patients with high expression of HSPb1 was 29.0%, although the difference was not significant ($p = 0.221$). These data suggests that HSPB1 is a potential target for future ESCC treatment.

4. Discussion

The conversion between activated and inactivated states of ezrin is closely related to the expansion and folding of the α-helical region (Ben-Aissa et al., 2012). The current most favored model regarding ERM protein activation is that the binding of ERM to PIP2 results in the release of C-ERMA from the FERM domain by inducing conformational changes, thus forming an open ERM monomer. Many studies have shown that ezrin has a high affinity for PIP2 in vitro (Niggli et al., 1995; Blin et al., 2008; Yonemura et al., 2002), and several lines of evidence also suggest the ERM proteins interact with PIP2 in vivo (Yonemura et al., 2002; Hao et al., 2009). However, how ezrin recruited to PIP2 remains unclear. Ezrin K253/254 and K262/263 are PIP2-binding sites, which are essential for the conformational activation of ezrin. When lysine is mutated to asparagine (K253/254N, K262/263N and K253/254/262/263N), the binding of ezrin to PIP2 is blocked. Our study showed that 1) HSPB1 bound to the α-helical region of ezrin and only interacted with inactivated ezrin (T567A), whereas there was no interaction between HSPB1 and the activated ezrin (T567D); 2) HSPB1 interacted with the ezrin binding to PIP2, because ezrin K253/254 N, K262/263 N and K253/254/262/263 N mutants significantly inhibited the interaction between ezrin and HSPB1; 3) HSPB1 knockdown inhibited ezrin activation (reduced ezrin T567 phosphorylation) and ezrin binding to F-actin. These data indicate that the interaction between HSPB1 and ezrin is important for the binding of ezrin to PIP2 to bring about the activation of ezrin. Silencing HSPB1 reduces the phosphorylation of ezrin at T567, suggesting that HSPB1 may promote the activation of ezrin or maintain the stability of the activated ezrin. The former is more credible, since HSPB1 only interacts with inactivated ezrin. We speculate that HSPB1, as a molecular chaperone, assists ezrin to bind to PIP2 and mediates ezrin activation, and eventually, affects the binding of ezrin to F-actin and cell migration.

Activated ERM proteins can bind many proteins residing in apical membranes, such as CD44 (Mori et al., 2008) and EBP50 (Reczek and Bretscher, 1998). These interactions provide the basis for local recruitment of protein networks and connect these networks with cytoskeleton to promote the reconstruction of cytoskeleton and membrane, thereby affecting cell migration. Ezrin knockdown downregulated the expression of connective tissue growth factor (CTGF) and cysteine-rich angiogenic inducer 61 (CYR61), which were target genes of TGF-β pathway, and decrease the phosphorylation of ERK/MAPK pathway, inhibiting the migration, growth and invasiveness in ESCC cells (Xie et al., 2009). In this study, we demonstrate that silencing HSPB1 reduces the phosphorylation of ezrin at T567, and inhibits the migration of ESCC cells (Fig. 3A–C, E–G). It is worth noting that the p-ERM (T567) antibody, which was used to detect the phosphorylation of the ezrin T567, also recognizes phosphorylation at radixin T564 and moesin T558. Ezrin, as a member of the ERM protein family, is very similar to radixin and moesin in structure, activation and function (Sauvanet et al., 2015). Therefore, HSPB1 knockdown may not only inhibit ezrin activation but also the activation of radixin and moesin, which would explain why overexpression of activated ezrin cannot restore cell migration from HSPB1 knockdown in ESCC cells. In addition, there are multiple phosphorylation sites in ezrin, such as ezrin S66, which also regulate cell migration (Li et al., 2017; Mak et al., 2012). The interaction of HSPB1 with phosphorylated ezrin at these sites may also affect cell migration. In sum, the malfunction of activated ezrin in HSPB1 knockdown cells is a result of a variety of factors.

When cells are stimulated by heat or other stresses, HSPB1 is phosphorylated at S78 and S82 and depolymerizes from a polymer to an oligomer, binding to cell microfilaments and preventing cells from undergoing apoptosis (Doshi et al., 2010; Katsogiannou et al., 2014). Overexpression of HSPB1 has been verified in a variety of tumors, such as prostatic carcinoma (Miyake et al., 2006) and mammary cancer (Mischak et al., 2010), promoting tumor formation and metastasis (Bruey et al., 2000; Garrido et al., 1998; Fanelli et al., 2008; Gibert et al., 2012). In this study, we found that patients with low expression of HSPB1 had higher five-year survival rate, suggesting that HSPB1 may be a potential therapeutic target and prognostic molecular marker for ESCC.

In summary, a novel ezrin interacting protein, HSPB1, facilitates the activation of ezrin by binding to the α-helical region of non-activated ezrin, thereby promoting movement of ESCC cells. Overexpression of HSPB1 is closely associated with poor prognosis of patients with ESCC.

Conflicts of interest

No potential conflicts of interest were disclosed.

Acknowledgements

We thank Dr. Stanley Li Lin from the Department of Cell Biology and Genetics of Shantou University Medical College for assistance in revising the manuscript. This work was supported by grants from the Natural Science Foundation of China-Guangdong Joint Fund (No.U0932001) and the National Natural Science Foundation of China (No.81172264, 81472613 and No. 81872372).

Appendix A. Supplementary data

Supplementary material related to this article can be found, in the online version, at doi:https://doi.org/10.1016/j.biocel.2019.05.005.

References

Adada, M., Canals, D., Hannun, Y.A., Obeid, L.M., 2014. Sphingolipid regulation of ezrin, radixin, and moesin proteins family: implications for cell dynamics. Biochim. Biophys. Acta 1841 (5), 727–737.

Ben-Aissa, K., Patino-Lopez, G., Belkina, N.V., Maniti, O., Rosales, T., Hao, J.J., Kruhlak, M.J., Knutson, J.R., Picart, C., Shaw, S., 2012. Activation of moesin, a protein that links actin cytoskeleton to the plasma membrane, occurs by phosphatidylinositol 4,5-bisphosphate (PIP2) binding sequentially to two sites and releasing an autoinhibitory linker. J. Biol. Chem. 287 (20), 16311–16323.

Blin, G., Margeat, E., Carvalho, K., Royer, C.A., Roy, C., Picart, C., 2008. Quantitative analysis of the binding of ezrin to large unilamellar vesicles containing phosphatidylinositol 4,5 bisphosphate. Biophys. J. 94 (3), 1021–1033.

Bruey, J.M., Paul, C., Fromentin, A., Hilpert, S., Arrigo, A.P., Solary, E., Garrido, C., 2000. Differential regulation of HSP27 oligomerization in tumor cells grown in vitro and in vivo. Oncogene 19 (42), 4855–4863.

Camp, R.L., Dolled-Filhart, M., Rimm, D.L., 2004. X-tile: a new bio-informatics tool for biomarker assessment and outcome-based cut-point optimization. Clin. Cancer Res. 10 (21), 7252–7259.

Doshi, B.M., Hightower, L.E., Lee, J., 2010. HSPB1, actin filament dynamics, and aging cells. Ann. N. Y. Acad. Sci. 1197, 76–84.

Fanelli, M.A., Montt-Guevara, M., Diblasi, A.M., Gago, F.E., Tello, O., Cuello-Carrion, F.D., Callegari, E., Bausero, M.A., Ciocca, D.R., 2008. P-cadherin and beta-catenin are useful prognostic markers in breast cancer patients; beta-catenin interacts with heat shock protein Hsp27. Cell Stress Chaperones 13 (2), 207–220.

Fievet, B.T., Gautreau, A., Roy, C., Del Maestro, L., Mangeat, P., Louvard, D., Arpin, M., 2004. Phosphoinositide binding and phosphorylation act sequentially in the activation mechanism of ezrin. J. Cell Biol. 164 (5), 653–659.

Garrido, C., Fromentin, A., Bonnotte, B., Favre, N., Moutet, M., Arrigo, A.P., Mehlen, P., Solary, E., 1998. Heat shock protein 27 enhances the tumorigenicity of immunogenic rat colon carcinoma cell clones. Cancer Res. 58 (23), 5495–5499.

Gary, R., Bretscher, A., 1995. Ezrin self-association involves binding of an N-terminal domain to a normally masked C-terminal domain that includes the F-actin binding site. Mol. Biol. Cell 6 (8), 1061–1075.

Gibert, B., Eckel, B., Gonin, V., Goldschneider, D., Fombonne, J., Deux, B., Mehlen, P., Arrigo, A.P., Clezardin, P., Diaz-Latoud, C., 2012. Targeting heat shock protein 27 (HspB1) interferes with bone metastasis and tumour formation in vivo. Br. J. Cancer 107 (1), 63–70.

Gould, K.L., Bretscher, A., Esch, F.S., Hunter, T., 1989. cDNA cloning and sequencing of the protein-tyrosine kinase substrate, ezrin, reveals homology to band 4.1. EMBO J. 8 (13), 4133–4142.

Hao, J.J., Liu, Y., Kruhlak, M., Debell, K.E., Rellahan, B.L., Shaw, S., 2009. Phospholipase C-mediated hydrolysis of PIP2 releases ERM proteins from lymphocyte membrane. J. Cell Biol. 184 (3), 451–462.

He, J.Z., Wu, Z.Y., Wang, S.H., Ji, X., Yang, C.X., Xu, X.E., Liao, L.D., Wu, J.Y., Li, E.M., Zhang, K., Xu, L.Y., 2017. A decision tree-based combination of ezrin-interacting proteins to estimate the prognostic risk of patients with esophageal squamous cell carcinoma. Hum. Pathol. 66, 115–125.

Katsogiannou, M., Andrieu, C., Rocchi, P., 2014. Heat shock protein 27 phosphorylation state is associated with cancer progression. Front. Genet. 5, 346.

Li, L.Y., Xie, Y.H., Xie, Y.M., Liao, L.D., Xu, X.E., Zhang, Q., Zeng, F.M., Tao, L.H., Xie, W.M., Xie, J.J., Xu, L.Y., Li, E.M., 2017. Ezrin Ser66 phosphorylation regulates invasion and metastasis of esophageal squamous cell carcinoma cells by mediating filopodia formation. Int. J. Biochem. Cell Biol. 88, 162–171.

Liu, W., He, J.Z., Wang, S.H., Liu, D.K., Bai, X.F., Xu, X.E., Wu, J.Y., Jiang, Y., Li, C.Q., Chen, L.Q., Li, E.M., Xu, L.Y., 2018. MASAN: a novel staging system for prognosis of patients with oesophageal squamous cell carcinoma. Br. J. Cancer.

Lv, G.Q., Zou, H.Y., Liao, L.D., Cao, H.H., Zeng, F.M., Wu, B.L., Xie, J.J., Fang, W.K., Xu, L.Y., Li, E.M., 2014. Identification of a novel lysyl oxidase-like 2 alternative splicing isoform, LOXL2 Deltae13, in esophageal squamous cell carcinoma. Biochem. Cell Biol. 92 (5), 379–389.

Mak, H., Naba, A., Varma, S., Schick, C., Day, A., SenGupta, S.K., Arpin, M., Elliott, B.E., 2012. Ezrin phosphorylation on tyrosine 477 regulates invasion and metastasis of breast cancer cells. BMC Cancer 12, 82.

Mischak, H., Allmaier, G., Apweiler, R., Attwood, T., Baumann, M., Benigni, A., Bennett, S.E., Bischoff, R., Bongcam-Rudloff, E., Capasso, G., Coon, J.J., D'Haese, P., Dominiczak, A.F., Dakna, M., Dihazi, H., Ehrich, J.H., Fernandez-Llama, P., Fliser, D., Frokiaer, J., Garin, J., Girolami, M., Hancock, W.S., Haubitz, M., Hochstrasser, D., Holman, R.R., Ioannidis, J.P., Jankowski, J., Julian, B.A., Klein, J.B., Kolch, W., Luider, T., Massy, Z., Mattes, W.B., Molina, F., Monsarrat, B., Novak, J., Peter, K., Rossing, P., Sanchez-Carbayo, M., Schanstra, J.P., Semmes, O.J., Spasovski, G., Theodorescu, D., Thongboonkerd, V., Vanholder, R., Veenstra, T.D., Weissinger, E., Yamamoto, T., Vlahou, A., 2010. Recommendations for biomarker identification and qualification in clinical proteomics. Sci. Transl. Med. 2 (46), 46ps42.

Miyake, H., Muramaki, M., Kurahashi, T., Yamanaka, K., Hara, I., Fujisawa, M., 2006. Enhanced expression of heat shock protein 27 following neoadjuvant hormonal therapy is associated with poor clinical outcome in patients undergoing radical prostatectomy for prostate cancer. Anticancer Res. 26 (2B), 1583–1587.

Mori, T., Kitano, K., Terawaki, S., Maesaki, R., Fukami, Y., Hakoshima, T., 2008. Structural basis for CD44 recognition by ERM proteins. J. Biol. Chem. 283 (43), 29602–29612.

Niggli, V., Andreoli, C., Roy, C., Mangeat, P., 1995. Identification of a phosphatidylinositol-4,5-bisphosphate-binding domain in the N-terminal region of ezrin. FEBS Lett. 376 (3), 172–176.

Pearson, M.A., Reczek, D., Bretscher, A., Karplus, P.A., 2000. Structure of the ERM protein moesin reveals the FERM domain fold masked by an extended actin binding tail domain. Cell 101 (3), 259–270.

Reczek, D., Bretscher, A., 1998. The carboxyl-terminal region of EBP50 binds to a site in the amino-terminal domain of ezrin that is masked in the dormant molecule. J. Biol. Chem. 273 (29), 18452–18458.

Sauvanet, C., Wayt, J., Pelaseyed, T., Bretscher, A., 2015. Structure, regulation, and functional diversity of microvilli on the apical domain of epithelial cells. Annu. Rev. Cell Dev. Biol. 31, 593–621.

Xie, J.J., Xu, L.Y., Xie, Y.M., Zhang, H.H., Cai, W.J., Zhou, F., Shen, Z.Y., Li, E.M., 2009. Roles of ezrin in the growth and invasiveness of esophageal squamous carcinoma cells. Int. J. Cancer 124 (11), 2549–2558.

Xie, J.J., Xu, L.Y., Wu, J.Y., Shen, Z.Y., Zhao, Q., Du, Z.P., Lv, Z., Gu, W., Pan, F., Xu, X.E., Xie, D., Li, E.M., 2010. Involvement of CYR61 and CTGF in the fascin-mediated proliferation and invasiveness of esophageal squamous cell carcinomas cells. Am. J. Pathol. 176 (2), 939–951.

Xie, J.J., Xu, L.Y., Wu, Z.Y., Zhao, Q., Xu, X.E., Wu, J.Y., Huang, Q., Li, E.M., 2011. Prognostic implication of ezrin expression in esophageal squamous cell carcinoma. J. Surg. Oncol. 104 (5), 538–543.

Yonemura, S., Matsui, T., Tsukita, S., Tsukita, S., 2002. Rho-dependent and -independent activation mechanisms of ezrin/radixin/moesin proteins: an essential role for polyphosphoinositides in vivo. J. Cell. Sci. 115 (Pt 12), 2569–2580.

Zeng, F.M., Wang, X.N., Shi, H.S., Xie, J.J., Du, Z.P., Liao, L.D., Nie, P.J., Xu, L.Y., Li, E.M., 2017. Fascin phosphorylation sites combine to regulate esophageal squamous cancer cell behavior. Amino Acids 49 (5), 943–955.

Zhang, X.D., Huang, G.W., Xie, Y.H., He, J.Z., Guo, J.C., Xu, X.E., Liao, L.D., Xie, Y.M., Song, Y.M., Li, E.M., Xu, L.Y., 2018. The interaction of lncRNA EZR-AS1 with SMYD3 maintains overexpression of EZR in ESCC cells. Nucleic Acids Res. 46 (4), 1793–1809.